



Experimental study of the Portevin-Le Chatelier effect under complex loading of Al-Mg alloy: procedure issues

Tatyana V. Tretyakova

Center of Experimental Mechanics, Perm National Research Polytechnic University, Russia
cem.tretyakova@gmail.com, <http://orcid.org/0000-0001-9445-5185>

Mikhail P. Tretyakov

Center of Experimental Mechanics, Perm National Research Polytechnic University, Russia
cem_tretyakov@mail.ru, <http://orcid.org/0000-0001-6146-6769>

Evgeniia A. Chechulina

Ural Research Institute of Composite Materials, Perm, Russia
zhenya-chechulina@yandex.ru, <https://orcid.org/0000-0003-4834-7911>

ABSTRACT. The aim of this work is to solve the methodological issues of the experimental study of the nucleation and propagation of deformation bands due to the Portevin-Le Chatelier effect under conditions of complex loading. It is of interest to determine the boundaries of unstable plastic deformation of the AMg6 alloy under complex loading conditions. A technique for controlling the loading process with a given rate of deformation intensity of materials has been worked out. Short stops of the loading process and unloading have an impact on the manifestation of the jerky flow. Stops and unloading reduce the strain level at which the diagram starts to manifest the effect Portevin-Le Chatelier. The experimental results show the evolution of inhomogeneous strain fields and local strain rates under conditions of manifestation of jerky flow during tension with torsion tests of Al-Mg alloy samples.

KEYWORDS. Jerky flow; the Portevin-Le Chatelier effect; Strain field; Plasticity; Digital image correlation technique; Aluminum-magnesium alloy.



Citation: Tretyakova, T. V., Tretyakov, M. P., Chechulina, E.A., Experimental study of the Portevin-Le Chatelier effect under complex loading of Al-Mg alloy: procedure issues, *Frattura ed Integrità Strutturale*, 58 (2021) 434-441.

Received: 09.05.2021

Accepted: 25.09.2021

Published: 01.10.2021

Copyright: © 2021 This is an open access article under the terms of the CC-BY 4.0, which permits unrestricted use, distribution, and reproduction in any medium, provided the original author and source are credited.

INTRODUCTION

Real conditions of operation and complex external thermomechanical influences determine the operation of the loaded elements of critical structures in the conditions of a complex stress state. There is a need to create the scientific basis for predicting the deformation ability and the limiting state of metals and alloys, taking into account



the phenomena of spatial heterogeneity and temporary instability of plastic deformation under given operating conditions. The effects of discontinuous fluidity lead to a significant decrease in strength and ductility, reduce the quality of the surface of the material, affect the technological process of processing [1-7 and etc.]. Macroscopic localization of the plastic flow as a result of the formation of deformation bands leads to the difference in thickness of the material and, as a result, to the formation of defects and premature failure. Aluminum-magnesium alloys exhibit a tendency to dynamic strain aging at relatively low homologous temperatures, which leads to the appearance of numerous stress discontinuities in the tensile curves. The manifestation of the jerky flow significantly reduces the strength and ductility of materials, and decreases the surface quality as well [8].

An urgent task of the experimental study of the PLC effect is to determine the region of existence of instability in order to exclude it from the real modes of processing products. In addition, of particular interest is the experimental study of inelastic deformation of structural materials, taking into account their processing in real technological processes, characterized by non-monotonicity and complexity of deformation paths, loading modes (including the imposition of monotonous and oscillating vibrational influences), and the properties of the loading system [9-12].

The vast majority of known experimental studies of the PLC effect were carried out under uniaxial (simple) loading. It is known that inelastic deformation processes are significantly affected by loading complexity. Moreover, the behavior of metals and alloys is significantly affected by the energy of the stacking fault [13, 14], which determines the tendency of edge dislocations to split. In view of the foregoing, it seems possible to suggest that the energy of the stacking fault and complex load also affect the occurrence and characteristics of intermittent ductility. The influence of complicated loading on the PLC effect [15-17], based on the physical analysis of dislocation deformation mechanisms, will manifest itself in the form of an increase in the intensity of the formation of barriers (for example, the Lomer - Cottrell), which, by assumption, will lead to an increase in the amplitude of loading jumps in the stress - strain diagram.

The aim of this work is to solve the methodological issues of experimental study of the regularities of the nucleation and propagation of deformation bands of localized plastic flow, determination of the boundaries of unstable plastic deformation of the AMg6 alloy under conditions of complex loading. The choice of the AMg6 alloy was determined by the importance of the problem of stability of its deformation behavior in connection with its wide application in aviation engineering, shipbuilding, chemical industry and transport engineering.

EXPERIMENTAL PROCEDURE

Material and specimen geometry

The structural aluminum-magnesium alloy in the form of a thick-walled pipe in the state of delivery ($\varnothing 28$ mm, wall thickness 5 mm) was selected as the material for the study. The chemical composition of the alloy in mass fractions according to GOST 4784-97 is presented in Tab. 1.

Al	Mg	Mn	Fe	Si	Zn	Ti	Cu	Be
92.55	6.12	0.84	0.27	0.17	0.005	0.039	0.001	0.005

Table 1: The chemical composition of the used alloy (%wt).

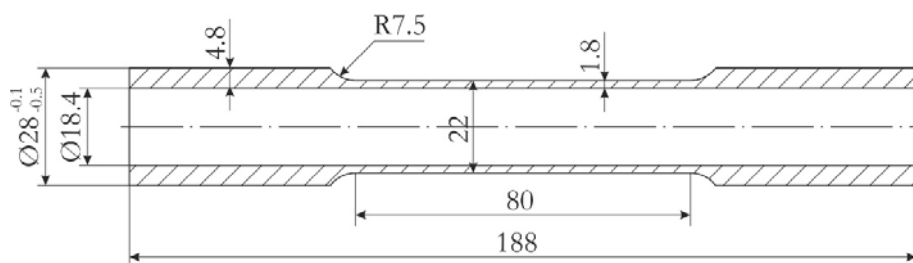


Figure 1: Sketch of a thin-walled tubular test specimen for tensile torsion tests.

In mechanical tests, thin-walled tubular specimens were used, a sketch of which is shown in Fig. 1. The specimens were manufactured on a numerically controlled chuck-center lathe in accordance with GOST 25.505-85. The samples satisfy the thin-walled condition, that is, the ratio of the wall thickness of the working part to the diameter is less than 0.1. To achieve

homogeneity of the microstructure and relieve residual stresses, samples of the Al-Mg alloy were annealed in a muffle furnace at 400 ° C for 3 hours and cooled in the furnace to room temperature.

Testing equipment and registration technique

In this work, to assess the stress-strain state and the characteristics of the deformation process, the values of the intensity of deformations and the intensity of the rates of deformations were used. The calculation of the intensity of deformations is made according to the following formula [18]:

$$\epsilon_i = \frac{\sqrt{2}}{3} \sqrt{(\epsilon_{11} - \epsilon_{22})^2 + (\epsilon_{22} - \epsilon_{33})^2 + (\epsilon_{33} - \epsilon_{11})^2 + 6 \times (\epsilon_{12}^2 + \epsilon_{23}^2 + \epsilon_{31}^2)}, \quad (1)$$

where $\epsilon_{11}, \epsilon_{22}, \epsilon_{33}$ – normal strain components, $\epsilon_{12}, \epsilon_{23}, \epsilon_{31}$ – components of shear deformations. For the case when only a tensile load and a torque act on a thin-walled tubular specimen, the formula for calculating the intensity of deformations can be written in the following form:

$$\epsilon_i = \frac{\sqrt{2}}{3} \sqrt{\frac{9}{2} \epsilon_{11}^2 + \frac{3}{2} \gamma_{12}^2}. \quad (2)$$

The strain rate intensity according to [11] is calculated using similar formulas, while strain rate components are used instead of strain components. The strain rate components for proportional loading are selected from the conditions that the strain rate intensity is constant and equal $\dot{\epsilon}_i = 5,4 \times 10^{-4}$ 1/s, as well as a fixed ratio of the shear angle and axial strain rate components $\dot{\gamma}_{12}/\dot{\epsilon}_{11} = 0,125$. As a result, the following velocities were obtained for the components of deformations: $\dot{\epsilon}_{11} = 5,385 \times 10^{-4}$ 1/s and $\dot{\gamma}_{12} = 0,675 \times 10^{-4}$ 1/s. In tests for complex loading at successive tension with torsion, tension and torsion, the rates of the deformation components corresponded to the given rate of the deformation intensity and are given in Tab. 2.

Components	Tension with torsion	Tension	Torsion
$\dot{\epsilon}_{11}$	$5.384 \cdot 10^{-4}$ 1/s	$5.4 \cdot 10^{-4}$ 1/s	0
$\dot{\gamma}_{12}$	$0.675 \cdot 10^{-4}$ 1/s	0	$9.35 \cdot 10^{-4}$ 1/s
$\dot{\epsilon}_i$	$5.4 \cdot 10^{-4}$ 1/s	$5.4 \cdot 10^{-4}$ 1/s	$5.4 \cdot 10^{-4}$ 1/s

Table 2: Values of velocities by deformation components for various types of tests.

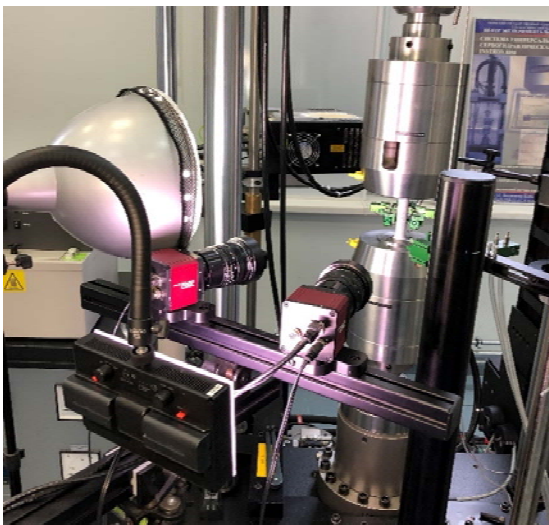


Figure 2: The biaxial servo-hydraulic test system Instron 8850 (left), the biaxial extensometer Epsilon 3550-025M (right).

Mechanical tests on tension, torsion and tension-torsion were carried out using the biaxial (tension/torsion) servo-hydraulic test system Instron 8850 (Fig. 2, a). The maximum loads are 100 kN in tension / compression and 1000 Nm in torsion. The travel ranges are ± 75 mm in the tension / compression axis and $\pm 45^\circ$ in the torsion axis. To fix the specimens in the testing system, hydraulic collet-type grippers were used. At the first stage of testing, registration of axial and shear deformations in the working part of the specimens was carried out by using a two-axis extensometer Epsilon 3550-025M (Fig. 2, b). Registration of inhomogeneous displacement and strain fields was carried out by using the Vic-3D digital image correlation measurement system (Fig. 2). The shooting of specimens was realized with a set of high-resolution cameras (Prosilica, 16 Mp), the shooting speed was 3 frames per second. The systems were synchronized with an analog-to-digital converter (NI USB-6251).

RESULTS

Methodology for tensile torsion test at discontinuous yield

However, the use of a hinged extensometer imposes some restrictions on the test methodology due to its limited range of strain measurement. In this regard, the original test procedure provided for stopping the loading process, unloading (or holding on load and torque) to reinstall the extensometer. The stop duration ranged from 30 s to 60 s. At the same time, it was found that after unloading (or suspension) of loading in the region of uniform deformation, further loading led to the manifestation of the effect of intermittent yield.

Fig. 3 shows the experimental diagrams in the coordinates load-elongation (left) and torque-twist angle (right), obtained under proportional tension with torsion of the sample up to an elongation of 3.5 mm (point 1), followed by unloading for reinstallation of the extensometer and further proportional loading. At point 2, the extensometer was reinstalled when the loading process was stopped without unloading. The data obtained demonstrate that with repeated proportional loading, the onset of non-uniform intermittent deformation is provoked.

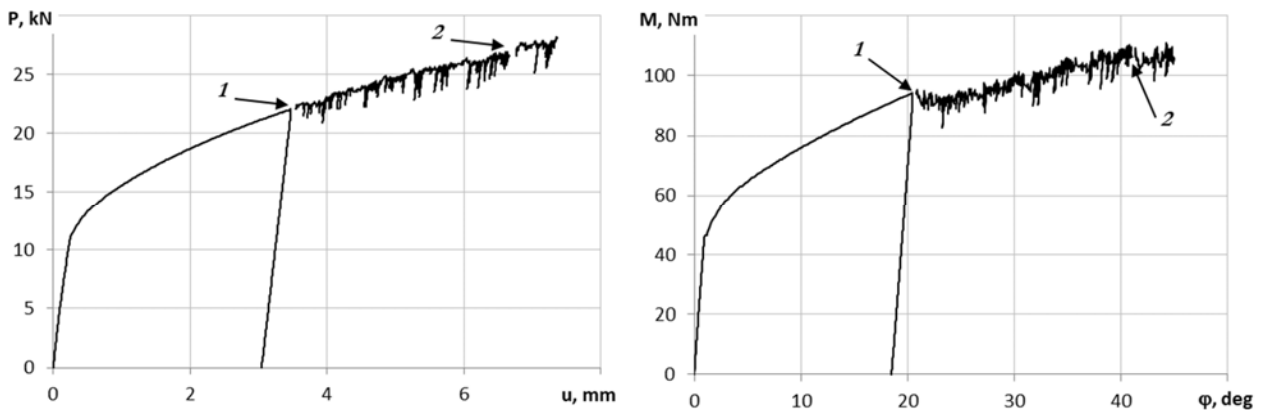


Figure 3: Deformation diagrams in the coordinates load-elongation (left) and torque-angle of twist (right), obtained under proportional tension with torsion of the sample up to an elongation of 3.5 mm (point 1), unloading and subsequent loading. Point 2 is to reset the extensometer when stopped without unloading.

In the next test, the stop for reinstallation of the extensometer was implemented at a lower value of the achieved elongation (extension of 2.5 mm), while no unloading was performed. However, even at this level of deformations after stopping with further proportional loading, a process of inhomogeneous intermittent deformation is provoked. Fig. 4 shows the experimental diagrams in the coordinates load-elongation (left) and torque-twist angle (b), obtained with proportional tension with torsion of the sample up to an elongation of 2.5 mm (point 1) for reinstallation of the extensometer and further proportional loading. At point 2, the extensometer was also reset when the loading process was stopped without unloading. Experimental data show that when the proportional loading process stops even at small values of plastic deformations, further loading leads to the occurrence of inhomogeneous intermittent plastic deformation processes. This is reflected in the recorded deformation diagrams in the form of the PLC effect. In this regard, it was decided to adapt the test methodology and carry out proportional loading of the samples with control using the built-in sensors of the testing system. This makes it possible to realize quasi-static loading up to the required values of axial and shear deformations without

interruptions in the process of plastic deformation. In order to achieve the strain rates, elongation rates and rotational angles shown in Tab. 2, the built-in transducers of the test system were determined from previous tests in the elastic section. The obtained speeds of the specified elongation and rotation angle are shown in Tab. 2.

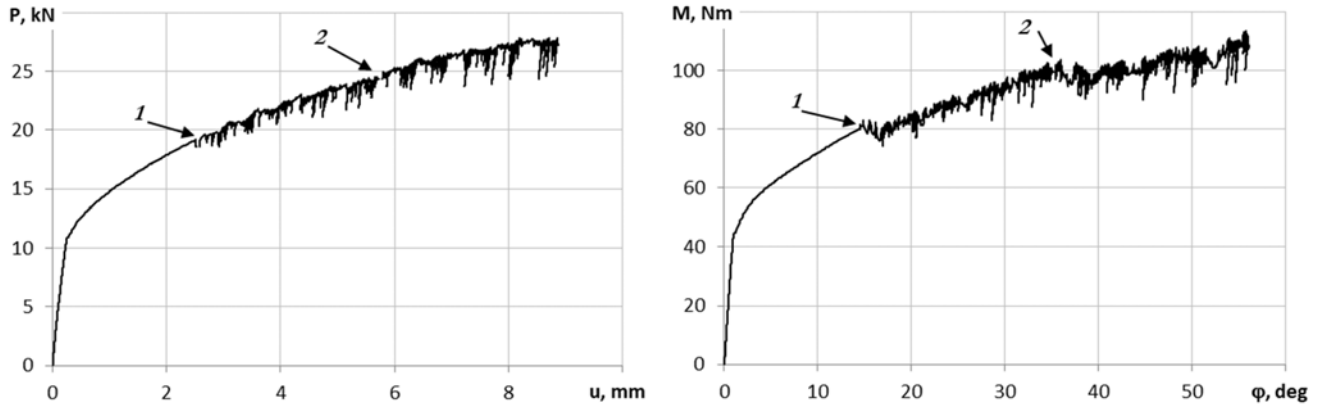


Figure 4: Deformation diagrams in coordinates load-elongation (left) and torque-twist angle (right), obtained under proportional tension with torsion of the sample up to an elongation of 2.5 mm (point 1) and subsequent loading. Point 2 - repositioning the extensometer when stopped without unloading.

Components	Tension with torsion	Tension	Torsion
\dot{u} [mm/s]	0.05332	0.05347	0
$\dot{\varphi}$ [grad/s]	0.31870	0	4.4146

Table 3: Values of elongation and rotation rates for various types of tests.

A quasi-static proportional tension-torsion tests were carried out with the loading parameters indicated in Tab. 3. The test was stopped at the loss of stability of the working part of the thin-walled tubular specimen. The test results in the form of diagrams in the coordinates load-elongation (left) and torque-twist angle (right) are shown in Fig. 5. The figure also shows the section of the transition from the process of homogeneous plastic to discontinuous deformation.

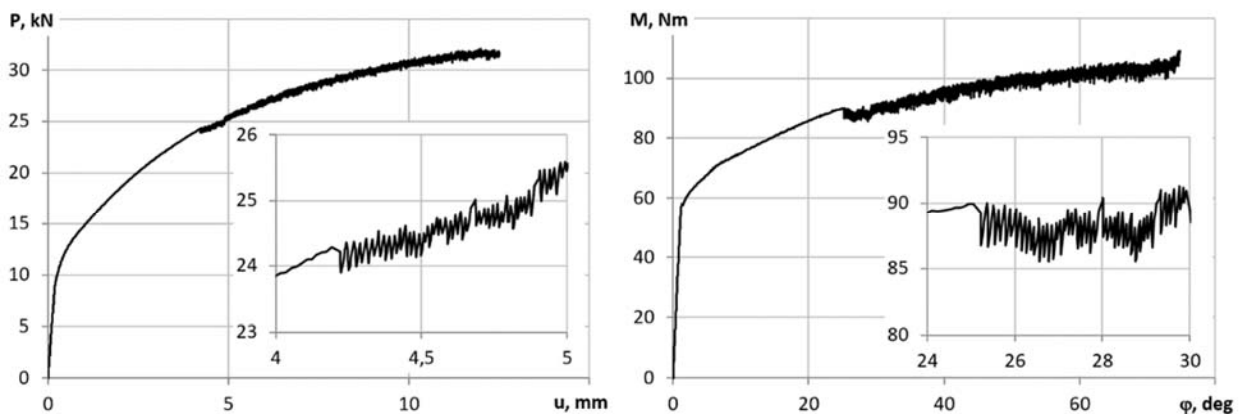


Figure 5: Diagrams of proportional quasi-static deformation of the specimen with control by the built-in sensors of the test system in the coordinates load-elongation (left) and torque-twist angle (right).

The Portevin-Le Chatelier effect during tension-torsion loading

The registration of strain distribution fields during plastic deformation of the samples was carried out with a Vic-3D Correlated Solutions non-contact three-dimensional optical system [19, 20]. The use of two cameras located at a certain

angle in the video system makes it possible to work not only with flat specimens, but also with cylindrical specimens, specimens of complex shape and structural elements. The use of this system makes it possible to obtain data on the distribution of normal and shear strain components on the surface of the working part of the specimen. Of particular interest is the analysis of the distribution of deformations and rates of deformation in the process of inhomogeneous discontinuous plastic flow. Distributions are plotted in the form of diagrams for different stages of the formation of bands of localized plastic deformation. Fig. 6 shows a set of plots of longitudinal strain (ϵ_{yy}), plotted at equal time intervals along the length of the specimen (along the Oy axis), the center of coordinates is located in the center of the working section. By analyzing the configuration of the longitudinal deformation profile [13], it is possible to track the moment of initiation of the process of macroscopic localization of plastic deformation due to the PLC bands.

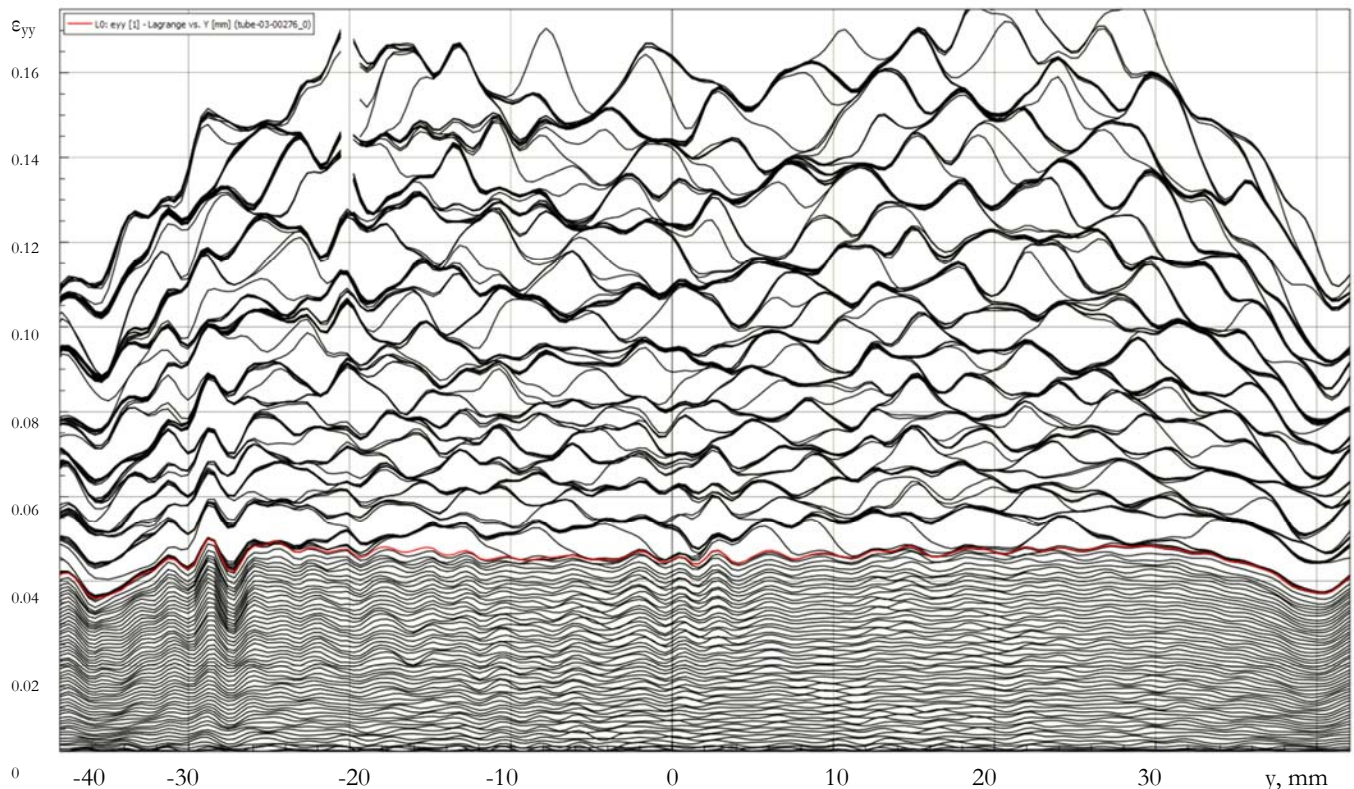


Figure 6: Series of plots of longitudinal deformations plotted at equal time intervals along the length of a thin-walled cylindrical specimen.

Inelastic deformation proceeds in a macro-uniform manner until the beginning of the manifestation of the effect of discontinuous flow. This is confirmed by a uniform increase in the level of longitudinal deformation, recorded by the video system (Fig. 6). It is of interest to consider in detail the process of the appearance of the first stress abrupt jump on the deformation diagram, which is accompanied by the initiation of the macrolocalization zone of the plastic flow.

Tensile torsion tests of thin-walled tubular samples of the AMg6 alloy were carried out under kinematic loading with a constant strain rate with control of axial displacements and torsion angle. The analysis of the spatio-temporal inhomogeneity of inelastic deformation during loading was carried out on the basis of the use of video system data, which made it possible to estimate the configuration of the PLC strips and the moment of the onset of the manifestation of the discontinuous yield effect.

ACKNOWLEDGES

This work was carried out by using the capabilities of a large unique scientific facility (UNU) ‘A set of test and diagnostic equipment for studying the properties of structural and functional materials under complex thermomechanical influences’, which is part of the Center of Experimental Mechanics, PNRPU (Perm, Russia). This work was supported by the Russian Science Foundation (No. 20-79-10235).

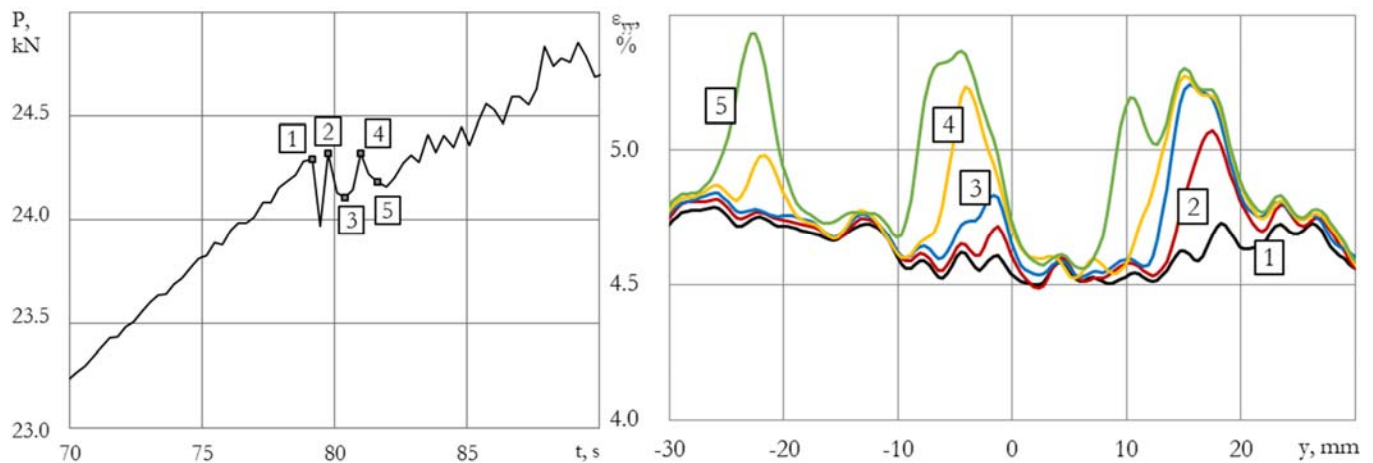


Figure 7: Section of the load-time diagram at the moment of initiation of the PLC effect (left) and a series of corresponding longitudinal deformation diagrams (right).

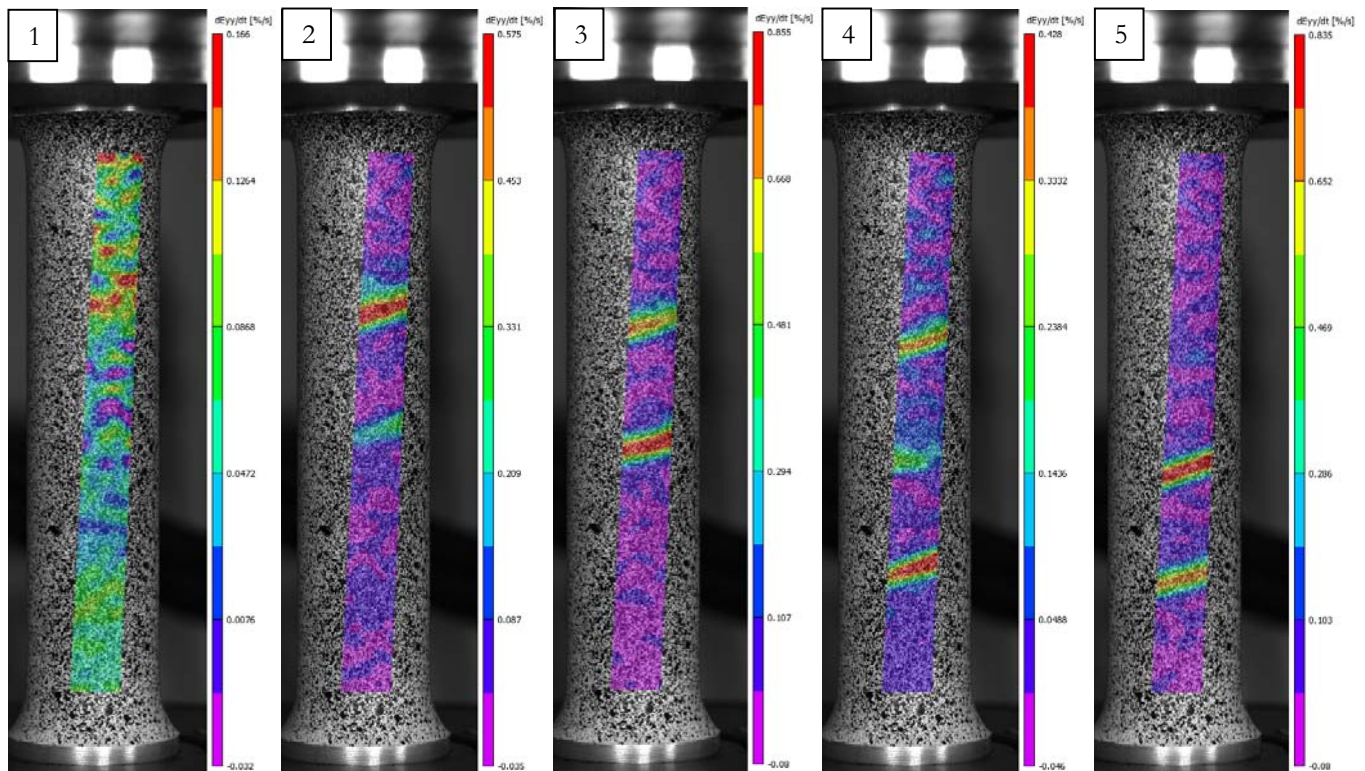


Figure 8: Evolution of inhomogeneous fields of local rates of longitudinal deformation on the surface of a thin-walled cylindrical specimen at the moment of initiation of the PLC effect (Fig. 7).

REFERENCES

- [1] Cottrell, A.H. (1953). A note on the Portevin-Le Chatelier effect, *Philosophical Magazine Series*, 44 (355), pp. 829–832. DOI: 10.1080/14786440808520347
- [2] Estrin, Y., Kubin, L.P. (1991). Plastic instabilities: phenomenology and theory, *Materials Science and Engineering, A*, 137, pp. 125–134. DOI: 10.1016/0921-5093(91)90326-I
- [3] Estrin, Y., Ling, C.P., McCormick, P.G. (1991). Localization of plastic flow: Spatial vs temporal instabilities, *Acta metal*, 39 (11), pp. 2943–2949. DOI: 10.1016/0956-7151(91)90110-M



- [4] McCormick, P.G. (1988). Theory of flow localization due to dynamic strain aging, *Acta Metall*, 36 (12), pp. 3061–3067. DOI: 10.1016/0001-6160(88)90043-0
- [5] Wang, X.G., Wang, L., Huang, M.X. (2017). Kinematic and thermal characteristics of Lüders and Portevin-Le Châtelier bands in a medium Mn transformation-induced plasticity steel, *Acta Materialia*, 124, pp. 17-29. DOI: 10.1016/j.actamat.2016.10.069
- [6] Krishtal, M.M. (2004). Instability and mesoscopic inhomogeneity of plastic deformation (analytical review). Part I. Phenomenology of yield drop and jerky flow, *Phys. Mesomech.*, 7 (5-6), pp. 5-26
- [7] Krishtal, M.M. (2004). Instability and mesoscopic inhomogeneity of plastic deformation (analytical review). Part II. Theoretical views on mechanisms of plastic deformation instability, *Phys. Mesomech.*, 7 (5-6), pp. 27-39
- [8] Bell J.F. (1973). Volume I: The Experimental Foundations of Solid Mechanics. Springer, Berlin. ISBN 978-3-540-13160-1.
- [9] Dietrich L., Socha G. (2012). Accumulation of damage in A336 GR5 structural steel subject to complex stress loading. *Strain*, 48, pp. 279-285. DOI: 10.1111/j.1475-1305.2011.00821.x
- [10] Feltner C.E., Laird C. (1967a). Cyclic stress-strain response of f.c.c. metals and alloys—I. Phenomenological experiments. *Acta Metallurgica*, 15, pp.1621-1632. DOI: 10.1016/0001-6160(67)90137-X
- [11] Tretyakova, T.V., Wildemann, V.E. (2017) Influence the loading conditions and the stress concentrators on the spatial-time inhomogeneity due to the yield delay and the jerky flow: study by using the digital image correlation and the infrared analysis, *Frattura ed Integrità Strutturale* 11 (42), pp. 303-314. DOI: 10.3221/IGF-ESIS.42.32
- [12] Tretyakova, T.V., Wildemann, V.E., Tretyakov, M.P. (2019) Investigation of the Portevin-Le Chatelier effect in metals under additional vibration impact by using the DIC-technique and the IR-analysis, *Procedia Structural Integrity* 18, pp. 837-842. DOI 10.1016/j.prostr.2019.08.233
- [13] Koneva, N.A., Trishkina, L., Cherkasova, T.V. (2017) Influence of stacking fault energy on the accumulation of dislocations during plastic deformation of polycrystalline copper-based alloys. *Letters on materials*, 7 (3), pp. 282-286.
- [14] Maksimkin, O.P. (2010) Packing faults, their energy and influence on the properties of irradiated metals and alloys, *Almaty*, P. 70.
- [15] Benallal A., Marquis D. (1988). Effects of non-proportional loadings in cyclic elasto-viscoplasticity: experimental, theoretical and numerical aspects, *Engineering Computations*, 5(3), pp. 241-247. DOI: 10.1108/eb023742
- [16] Benallal A., Le Gallo P., Marquis D. (1989). An experimental investigation of cyclic hardening of 316 stainless steel and of 2024 aluminium alloy under multiaxial loadings. *Nuclear Engineering and Design*, 114, pp. 345-353. DOI: 10.1016/0029-5493(89)90112-X
- [17] Borodii M. V., Stryzhalo V. O., Kucher M. K., Danylchuk E. L., and Adamchuk M. P. (2014). An experimental study of ratcheting effect under multiaxial proportional loading. *Strength of Materials*, 46(1), pp. 97-104. DOI: 10.1007/s11223-014-9520-3
- [18] Ilyushin, A.A. (2004). *Plasticity. Part 1: Elastic-plastic deformations*, Moscow, Logos. ISBN 5-94010-377-4.
- [19] Sutton, M.A., Orteu, J.-J., Schreier, H. (2009) *Image Correlation for Shape, Motion and Deformation Measurements*, University of South Carolina, Columbia, SC, USA, Springer. DOI: 10.1007/978-0-387-78747-3.
- [20] Tretyakova, T.V., Wildemann, V.E. (2018) Plastic strain localization and its stage in Al-Mg alloys. *Physical Mesomechanics* 21 (4), pp. 314-319. DOI: 10.1134/S1029959918040057